Unravelling of a mechanism of resistance to colistin in Klebsiella pneumoniae using atomic force microscopy

Cécile Formosa-Dague, M. Herold, C Vidaillac, R. E. Duval, Etienne Dague

Journal of Antimicrobial Chemotherapy Advance Access published May 27, 2015

J Antimicrob Chemother
doi:10.1093/jac/dkv118

Journal of Antimicrobial Chemotherapy

Unravelling of a mechanism of resistance to colistin in *Klebsiella pneumoniae* using atomic force microscopy

C. Formosa[1–4], M. Herold[3–5], C. Vidaillac[3,4]†, R. E. Duval[3–5] and E. Dague[1,2]*

[1]*CNRS, LAAS, 7 avenue du Colonel Roche, F-31400 Toulouse, France;* [2]*Université de Toulouse, LAAS, F-31400 Toulouse, France;* [3]*CNRS, UMR 7565, SRSMC, F-54506 Vandœuvre-lès-Nancy, France;* [4]*Université de Lorraine, UMR 7565, SRSMC, Faculté de Pharmacie, F-54001 Nancy, France;* [5]*ABC Platform®, F-54001 Nancy, France*

*Corresponding author. Tel: +0033-5-61-33-78-41; E-mail: edague@laas.fr
†Present address: CRP-Santé, Clinical and Epidemiological Investigation Center (CIEC), 1A rue Thomas Edison, L1445 Strassen, Luxembourg.

Received 8 September 2014; returned 13 October 2014; revised 7 April 2015; accepted 8 April 2015

Objectives: In this study we focused on the mechanism of colistin resistance in *Klebsiella pneumoniae*.

Methods: We used two strains of *K. pneumoniae*: a colistin-susceptible strain (*K. pneumoniae* ATCC 700603, KpATCC) and its colistin-resistant derivative (KpATCCm, MIC of colistin 16 mg/L). We performed a genotypic analysis based on the expression of genes involved in LPS synthesis and L-Ara4N moiety addition. We also explored the status of the *mgrB* gene. Then, a phenotypic analysis was performed using atomic force microscopy (AFM). The Young modulus was extracted from force curves fitted using the Hertz model, and stiffness values were extracted from force curves fitted using the Hooke model.

Results: We failed to observe any variation in the expression of genes implicated in LPS synthesis or L-Ara4N moiety addition in KpATCCm, in the absence of colistin or under colistin pressure (versus KpATCC). This led us to identify an insertional inactivation/mutation in the *mgrB* gene of KpATCCm. In addition, morphology results obtained by AFM showed that colistin removed the capsule from the susceptible strain, but not from the resistant strain. Nanomechanical data on the resistant strain showed that colistin increased the Young modulus of the capsule. Extend force curves recorded on top of the cells allowed us to make the following hypothesis about the nanoarchitecture of the capsule of the two strains: KpATCC has a soft capsule consisting of one layer, whereas the KpATCCm capsule is harder and organized in several layers.

Conclusions: We hypothesize that capsular polysaccharides might be implicated in the mechanism of colistin resistance in *K. pneumoniae*, depending on its genotype.

Keywords: *K. pneumoniae*, colistin resistance, gene expression, capsules, atomic force microscopy

Introduction

Klebsiella pneumoniae, a member of the Enterobacteriaceae family, has been recognized for more than 100 years as a cause of community-acquired pneumonia.[1] However, the vast majority of *Klebsiella* infections are associated with hospitalization; urinary tract, bloodstream, lung as well as abdominal cavity infections have now become common. Numerous virulence factors have been described for *K. pneumoniae*, such as extracellular capsules. These are essential for the species' virulence, since the capsular material forms thick bundles of fibrillous structures that cover the bacterial surface in massive layers.[2] This protects the bacteria from phagocytosis and prevents killing by bactericidal serum factors.[3] Another important feature of *K. pneumoniae* is its ability to resist a large number of antibiotics through multiple mechanisms (production of enzymes, lack of permeability and efflux pumps). For example, within a few years after the introduction of cephalosporins, *K. pneumoniae* strains within hospitals were shown to produce β-lactamases able to inactivate these agents. These β-lactamases were in fact ESBLs, and are plasmid-mediated enzymes that hydrolyse oxyimino-β-lactams. Because these plasmids are mobile genetic elements, they spread and evolve rapidly;[4] they now also carry genes for resistance to other antibiotics, including aminoglycosides, chloramphenicol and sulphonamides. Therefore, *K. pneumoniae* strains containing these plasmids are MDR.[2,3,5] However, many ESBLs are readily inhibited by the commercially available β-lactamase inhibitors (clavulanic acid, tazobactam and sulbactam),[6] which serve as an important phenotypic test to identify ESBLs. In this study, we have specifically worked on the well-characterized *K. pneumoniae* ATCC 700603 strain, a clinical isolate obtained from a patient in the USA in 1994, which produces an ESBL called SHV-18.[7–9]

Because this ESBL is sensitive to clavulanic acid, this strain has been used as a reference strain for quality control in ESBL detection.

Management and treatment of ESBL-producing *K. pneumoniae* infections can be challenging. Currently, carbapenems are the only class of antibiotics that have consistently been effective against ESBL-producing *K. pneumoniae*. However, bacteria have developed carbapenemases (KPCs), which are ESBL-like enzymes that confer resistance to extended-spectrum cephalosporins and carbapenems.[1,6,10] Therefore, clinicians have had to turn to an old antibiotic of the polymyxin class, colistin, as a last-resort agent for the treatment of infections caused by MDR *K. pneumoniae*.[11] Polymyxins are cyclic lipodecapeptides that are strongly cationic. They were discovered as early as 1947[12] and were widely used at that time. However, following reports on nephrotoxicity and neurotoxicity in the 1970s, they were largely replaced by other, less toxic antibiotics.[13,14] Polymyxin B and polymyxin E (colistin) are the main antibiotics of this group, and the only ones used clinically. They are bactericidal and act rapidly and specifically on Gram-negative bacteria. Here, we have focused on colistin, which, like polymyxin B, has as its initial target the LPS of the outer membrane of Gram-negative bacteria. Because of its positive charges, colistin interacts electrostatically with LPS and competitively displaces divalent cations from the phosphate groups of lipid A of LPS.[15] This results in a change in the permeability of the cell wall, leakage of cell contents and subsequently cell death.[15,16] However, some authors argue that interaction with membranes is a part of the activity of polymyxin but not actually the lethal event.[17] Therefore, the precise mechanism of action of colistin remains contentious,[18] especially for capsulated bacterial species such as *K. pneumoniae*. Mechanisms resulting in decreased susceptibility to colistin are also unclear, and only two mechanisms of resistance, involving the modification of the extracellular capsule or the initial target of colistin, LPS, are currently recognized.[11] The main and most effective modification of LPS in *K. pneumoniae* involves the addition of the L-Ara4N (4-amino-4-deoxy-L-arabinose) moiety to lipid A,[19] which is mediated by the two-component systems PmrA/PmrB and PhoP/PhoQ.[20,21] This modification of the lipid A confers a less negative charge on the bacterial LPS, which leads to colistin resistance.[22] Recently, another mechanism of colistin resistance was discovered; it involves mutation/inactivation of the *mgrB* gene. In *K. pneumoniae*, the disruption of *mgrB* can up-regulate the PhoP/PhoQ system and the operon *arnBCADTEF*, responsible for the addition of the L-Ara4N moiety to lipid A.[23] Therefore, the *mgrB* gene has been described as a key target for acquired resistance to colistin.[24]

In this study, we investigated these two main mechanisms of colistin resistance in *K. pneumoniae*, using *K. pneumoniae* ATCC 700603 as a control strain and its colistin-resistant derivative, KpATCCm. To carry out this study, we first measured the level of expression of genes involved in the synthesis of LPS (*lpxA*, *lpxC* and *msbA*) and those involved in the synthesis of the L-Ara4N moiety (*pmrA*, *pmrB*, *pmrD*, *phoP*, *phoQ* and *arnT*) in both colistin-susceptible and colistin-resistant strains, with and without colistin for KpATCCm. We then investigated whether the *mgrB* gene was inactivated in the colistin-resistant strain. In a second part of the study, we used atomic force microscopy (AFM) to compare the surface properties of the extracellular capsule of *K. pneumoniae* ATCC 700603 and of KpATCCm, as well as their respective responses under colistin pressure in order to understand the mechanism of colistin resistance from the 'outside'. Since its invention in 1986,[25] AFM has developed into a powerful technology in biology,[26] especially to probe the effects of antimicrobial drugs on live bacteria or fungi.[27–30] Although the effects of colistin have already been shown by AFM on cells of *Pseudomonas* and *Acinetobacter baumannii*,[31–33] no work has been performed on live cells of *K. pneumoniae* using AFM in liquid conditions. The results of this original study combine both a genotypic and a phenotypic analysis of mechanisms of colistin resistance in KpATCCm and under colistin pressure.

Materials and methods

Bacterial growth conditions

The bacteria *K. pneumoniae* ATCC 700603 and its colistin-resistant derivative KpATCCm (ABC Platform® Bugs Bank) were stocked at −80°C, revivified on cation-adjusted Mueller–Hinton agar (BD, 211438) and grown in CAMHB (BD, 212322) for 24 h at 37°C. Antibiograms of the two strains are presented in Table S1 (available as Supplementary data at *JAC* Online).

Colistin treatment

MICs of colistin sulphate salt (Sigma-Aldrich, C4461-1G) were calculated for each strain according to the macrodilution method provided by the CLSI.[34] For *K. pneumoniae* ATCC 700603, the MIC of colistin was found to be 0.5 mg/L and that for KpATCCm was found to be 16 mg/L. These results were confirmed by antibiograms performed using an automated Vitek 2 system (bioMérieux, France) (Table S1). For gene expression experiments, RNAs were isolated from bacterial cells grown in CAMHB containing colistin at a concentration of 0.25×MIC or 0.5×MIC at 37°C to mid-log. For AFM experiments, bacteria were grown in CAMHB containing colistin at a concentration of 0.5×MIC or 0.75×MIC for 18–20 h at 37°C.

Genomic characterization and gene expression

RNAs were extracted using the RNeasy® Plus Mini Kit (Qiagen, 74136) and RNA concentration was measured at 260 nm using a NanoPhotometer® P-class (Implen, Munich, Germany). Reverse transcription was performed using the iScript™ cDNA Synthesis Kit (Bio-Rad, 170-8891). Sequences of primers were designed using Primer 3 and are listed in Table 1. No quantitative PCR (qPCR) reaction was performed for the *mgrB* gene. PCR products were analysed by gel electrophoresis. A molecular marker (EZ Load 100 bp molecular ruler, Bio-Rad, 170-8352) that includes 100–1000 bp in exact 100 bp increments was used. For the other genes, qPCR was performed using SsoAdvanced SYBR Green Supermix (Bio-Rad, 172-5264) on a CFX96 thermocycler (Bio-Rad). *16S* was used as the reference gene and efficacy was determined for each annealing temperature. Analyses were carried out in triplicate in three independent experiments. The data were stored and reprocessed according to the Pfaffl method with the associated software (Bio-Rad CFX Software Manager™ v2.1, Bio-Rad, Marnes la Coquette, France).

Sample preparation for AFM experiments

Bacterial cells were concentrated by centrifugation (4500 **g**, 3 min), washed twice in 1× PBS (Sigma, P3813-10PAK, filtered on 0.22 μm filters), resuspended in 1× PBS to a concentration of ∼10^8 cells/mL and immobilized on polyethylenimine (PEI; Fluka P3142-100 mL)-coated glass slides (prepared as described elsewhere[35]). Briefly, freshly oxygen-activated glass slides were covered with 0.2% PEI solution in deionized water and left for incubation overnight. Then the glass slides were rinsed with 20 mL of Milli-Q water and nitrogen dried. A total of 1 mL of the bacterial

Table 1. Primers used in this study

Gene name	Forward primer (F) (5′→3′)	Reverse primer (R) (5′→3′)	Accession number/reference
16S	TCA-TGG-CTC-AGA-TTG-AAC-GCT	TGC-GGT-ATT-AGC-TAC-CGT-TTC-C	NC_009648
lpxA	CCA-CAC-CAA-AAT-CGG-CCG-TGA	CCA-ACC-ATA-ACG-TGT-GAG-CCA	NC_009648
lpxC	TCA-CAC-TGA-CGT-TAC-GCC-CTG	CAT-CTT-CGA-CGC-GAA-CCG-TCT-C	NC_009648
msbA	CGG-GCT-AAT-CGT-AGC-GGC-GGT-G	TAA-TCG-ATG-CCC-CTT-CGC-GGA-C	NC_009648
pmrA	ATC-TGC-GCC-TTA-ACG-TCA-CT	ATG-CAC-TTC-CAG-GGT-ATT-GG	A79E_3435 CDS T02213
pmrB	AGA-TGA-CCA-CCA-GCA-TTT-CC	GAG-ACG-ACG-GTC-TCG-TTT-TC	KPN_00806 CDS T00566
pmrD	AAA-GTA-CAG-GAC-AAC-GCT-TCG	CAA-CGC-TCG-CTG-CTA-TAA-TG	KPN_02444 CDS T00566
phoP	TCA-GGT-TTT-CCG-GGA-TGT-CG	CGA-ATT-GCG-CTG-ATG-AAG-GG	HF536482
phoQ	CAC-CAT-ATA-GCT-GCG-CTT-GA	GCA-ATG-GCT-TCC-ATG-AGA-TT	HF536482
arnT	CCG-TTT-GCT-TTG-GCA-ACC-CGA	CAC-CCC-AGA-AGC-TGC-ACA-TCG	NC_009648
mgrB	TTA-AGA-AGG-CCG-TGC-TAT-CC	AAG-GCG-TTC-ATT-CTA-CCA-CC	[23]

suspension was then applied to the PEI-coated glass slide, allowed to stand for 1 h and rinsed with 1× PBS.

AFM experiments

Images were recorded in 1× PBS in the Quantitative Imaging™ mode available on the Nanowizard III AFM (JPK Instruments, Berlin, Germany), with MLCT AUWH cantilevers (nominal spring constant 0.01 N/m; Bruker, USA) at an applied force of 1 nN, with a z length between 2 and 3 μm and an approach–retract speed between 130 and 250 μm/s. Cantilever spring constants were measured prior to each experiment using the thermal noise method.[36] Force curves were recorded in force volume mode at an applied force of 2.0 nN. Data were processed using JPK data processing software (JPK Instruments, Berlin, Germany). For nanomechanical data, the Hertz model was used to extract Young modulus values and the Hooke model to extract stiffness values. The Hertz model gives the force F as a function of the indentation (δ) and the Young modulus (E) according to the equation $F=(2.E.\tan\alpha)/(\pi.(1-\nu^2)).\delta^2$, where α is the tip opening angle (35°) and ν the Poisson ratio (arbitrarily assumed to be 0.5).[37] The Hooke model considers the couple cantilever/cell wall as a spring. The stiffness of the cell wall (k_{cell}) is therefore determined from the slope of the linear portion of the raw force curves, according to $k_{cell}=k(s/1-s)$, where s is the experimentally accessible slope of the compliance region reached for sufficient loading forces and k is the cantilever spring constant.[38]

Results

Colistin resistance in KpATCCm is mediated by mgrB inactivation

We first investigated the expression of the genes involved in both the constitutive pathway of LPS synthesis and the addition of the L-Ara4N moiety. The results are presented in Table 2, and show that whatever the strain studied (colistin-resistant KpATCCm or colistin-susceptible KpATCC 700603), no modification of expression was observed in any of the gene groups analysed (i.e. LPS genes or L-Ara4N genes). This observation was also true upon treatment of the colistin-resistant KpATCCm strain with different concentrations of colistin (i.e. 0.25×MIC or 0.5×MIC) (Table 2). Therefore, in order to understand the genetic cause of the resistance of KpATCCm, we decided to study the status of the *mgrB* gene. To this end, the *mgrB* gene was amplified by PCR both in KpATCC and in its colistin-resistant derivative, KpATCCm. Amplicons were then subsequently analysed by gel electrophoresis (Figure 1). After migration, we observed that the amplicons of KpATCCm migrated less than those of KpATCC, which indicates that they are larger than those of KpATCC. Therefore, we concluded that, for KpATCCm, the *mgrB* gene presents an insertion, estimated to be ∼1000 bp (Figure 1). These results thus led us to conclude that colistin resistance in KpATCCm is mediated, at least in part, by *mgrB* inactivation.

Table 2. Monitoring of gene expression in KpATCCm, KpATCCmc$_{1/4}$ and KpATCCmc$_{1/2}$ compared with KpATCC

	Relative normalized expression ± SD			
	KpATCC	KpATCCm	KpATCCmc$_{1/4}$	KpATCCmc$_{1/2}$
lpxA	1	0.10 ± 0.57	0.01 ± 0.01	0.05 ± 0.02
lpxC	1	0.08 ± 0.43	0.03 ± 0.01	0.04 ± 0.02
msbA	1	0.06 ± 0.32	0.01 ± 0.00	0.04 ± 0.02
pmrA	1	0.17 ± 0.64	0.01 ± 0.00	0.00 ± 0.00
pmrB	1	0.12 ± 0.43	0.00 ± 0.00	0.01 ± 0.01
pmrD	1	0.09 ± 0.34	0.01 ± 0.01	0.04 ± 0.02
phoP	1	0.12 ± 0.45	0.01 ± 0.00	0.01 ± 0.01
phoQ	1	0.11 ± 0.41	0.01 ± 0.00	0.00 ± 0.00
arnT	1	0.12 ± 0.51	0.01 ± 0.01	0.06 ± 0.03

Colistin removes the capsule from the susceptible strain

In the second part of this study we chose to use AFM to evaluate the morphological and nanomechanical differences between the colistin-susceptible strain and the colistin-resistant derivative strain. *K. pneumoniae* ATCC 700603 was first probed in native conditions or under colistin treatment, with AFM used in the Quantitative Imaging™ mode.[39] Figure 2 presents the morphological modifications of the bacteria submitted to colistin treatment. The height image in Figure 2(a) shows two bacterial cells surrounded by their capsule in the absence of colistin; the cross-section data show

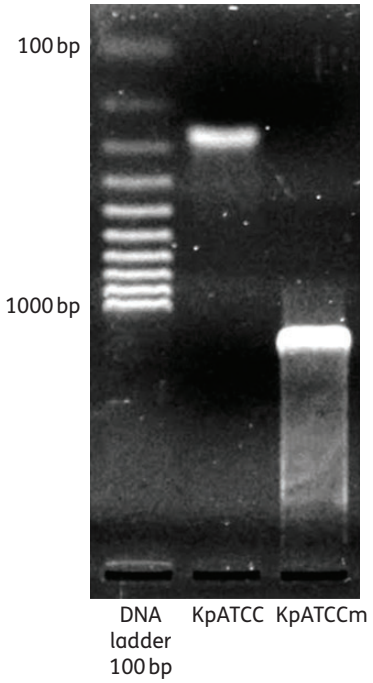

Figure 1. Gel electrophoresis of *mgrB* amplicons of KpATCC and KpATCCm.

that bacteria are 0.88 ± 0.11 μm high and 1.12 ± 0.15 μm wide, whereas the capsule is 0.56 ± 0.09 μm high but covers a surface 3.46 ± 0.28 μm in width (Figure 2b, values measured on five cells from three independent cultures). Regarding the extend force curves obtained on untreated cells, at a high applied force (2 nN), 81.3% of them (n = 5120) showed a spike that could correspond to the moment where the tip touches the capsule and moves through it, then through the bacterial cell, before reaching the glass slide (linear portion of the force curve) (Figure 2c). When cells were treated with colistin, at either 0.5×MIC (0.25 mg/L; Figure 2d–f) or 0.75×MIC (0.375 mg/L; Figure 2g–i), the capsule was no longer visible around the cells, which was confirmed by the cross-sections showing only the bacterial profile, with a height of 0.88 ± 0.06 μm and a width of 1.13 ± 0.11 μm (values measured on 10 cells from six independent cultures). The extend force curves recorded on these cells did not display a spike, allowing us to hypothesize that these spikes correspond to the rupture of the capsule by the AFM tip.

Colistin-resistant strain KpATCCm displays a different capsular organization

In the case of the colistin-resistant derivative of *K. pneumoniae* ATCC 700603 (i.e. KpATCCm), as can be seen on the height images in Figure 3(a, d and g), this strain did not show any adverse

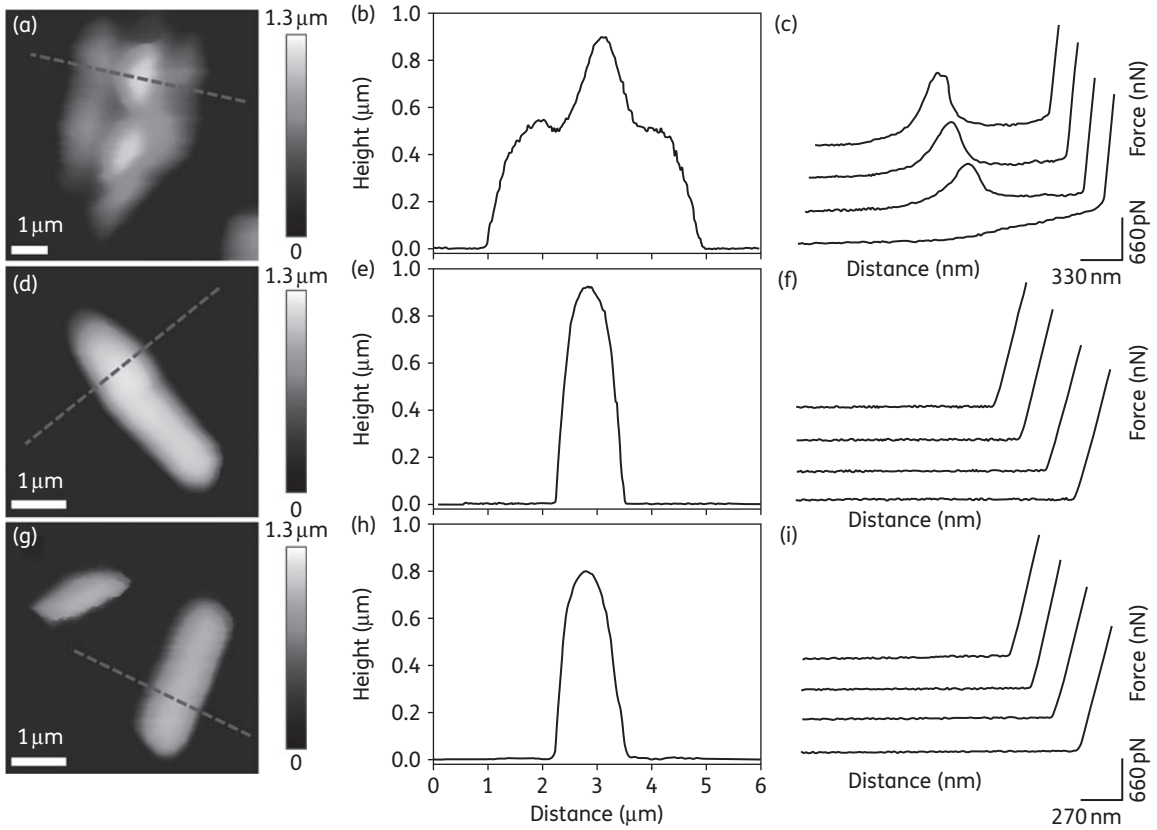

Figure 2. Imaging of *K. pneumoniae* ATCC 700603 cells. Height image of *K. pneumoniae* ATCC 700603 cells in native conditions (a), treated with colistin at 0.5×MIC (0.25 mg/L) (d) or treated with colistin at 0.75×MIC (0.375 mg/L) (g). (b, e and h) Cross-sections recorded along the broken lines in (a), (d) and (g), respectively. (c, f and i) Representative extend force curves recorded on small areas on top of cells presented in (a), (d) and (g), respectively. In each condition, force curves were recorded on five cells from three independent cultures (total of 5120 force curves per condition).

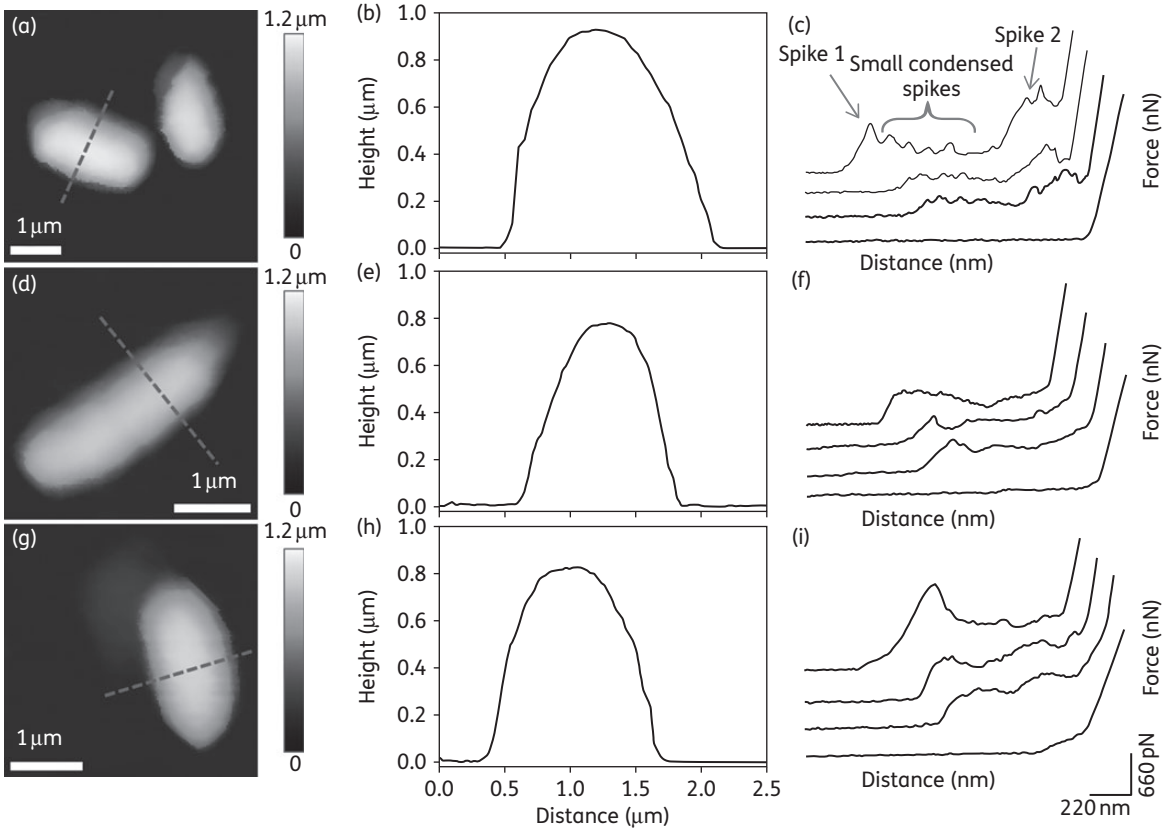

Figure 3. Imaging of *K. pneumoniae* colistin-resistant cells. Height image of *K. pneumoniae* colistin-resistant cells in native conditions (a), treated with colistin at 0.5×MIC (8 mg/L) (d) or treated with colistin at 0.75×MIC (12 mg/L) (g). (b, e and h) Cross-sections recorded along the broken lines on (a), (d) and (g), respectively. (c, f and i) Representative extend force curves recorded on small areas on top of cells presented in (a), (d) and (g), respectively. In each condition, force curves were recorded on five cells from three independent cultures (total of 5120 force curves per condition).

morphological changes after colistin treatment. Indeed, the cross-sections in Figure 3(b, e and h) show the same profile in the three different conditions: native or colistin treatment at 0.5×MIC (8 mg/L) or at 0.75×MIC (12 mg/L). The bacteria were 0.83 ± 0.06 µm high and 1.50 ± 0.11 µm wide, thus larger than the susceptible strain (values measured on 15 cells from nine independent cultures). It was at this stage that differences were first observed between the two strains. Even in native conditions, unlike KpATCC, KpATCCm did not have a capsule covering a large surface area. However, since KpATCCm cells were wider than susceptible strain cells, we can conclude that its capsule had a different morphology and was tightly bound to the bacterial cell wall. But the most interesting data obtained on KpATCCm cells were the extend force curves, presented in Figure 3(c, f and i). In native conditions, force curves displayed two spikes. After the first one on the left of the force curve (the one that was further away from the contact point), small condensed spikes were visible, suggesting that successive layers were ruptured by the AFM tip. When cells were treated with colistin the force curves presented the same profile, except that the small condensed spikes were not observed after the first spike, meaning that the several layers observed in native conditions were no longer present. In the three conditions mentioned earlier in this paragraph, the linear portions of the force curves corresponded to the contact of the tip with the glass slide, as force curves recorded on the glass slide with the same tip presented the same slope (data not shown). At this stage, the morphology data and the extend force curves recorded on cells of the susceptible and resistant strains of *K. pneumoniae* demonstrated that colistin was able to remove the capsule from the bacteria only in the case of the susceptible strain, and that the two strains presented a different capsular organization that could be probed using force spectroscopy. However the force curves of treated KpATCCm cells indicated that this capsular organization was lost upon treatment. We then investigated the effects of colistin on the nanomechanical properties of the cells.

Colistin modifies the nanomechanical properties of KpATCC and KpATCCm

Figure 4 presents the nanomechanical results obtained on the susceptible strain of *K. pneumoniae*. In native conditions, extend force curves obtained on cells, converted into indentation curves (Figure 4b, grey line) and fitted through the Hertz model (Figure 4b, empty circles) indicate, according a first interpretation of the force curves, to the stiffness of the capsule. Stiffness values measured on five cells from three independent cultures were on average of 3.6 ± 1.0 kPa (Figure 4a). However, when cells were treated with colistin, whatever the dose, force curves showed only a few nanometres of indentation and could not be fitted using the Hertz model. After verifying that the slope of these force curves was

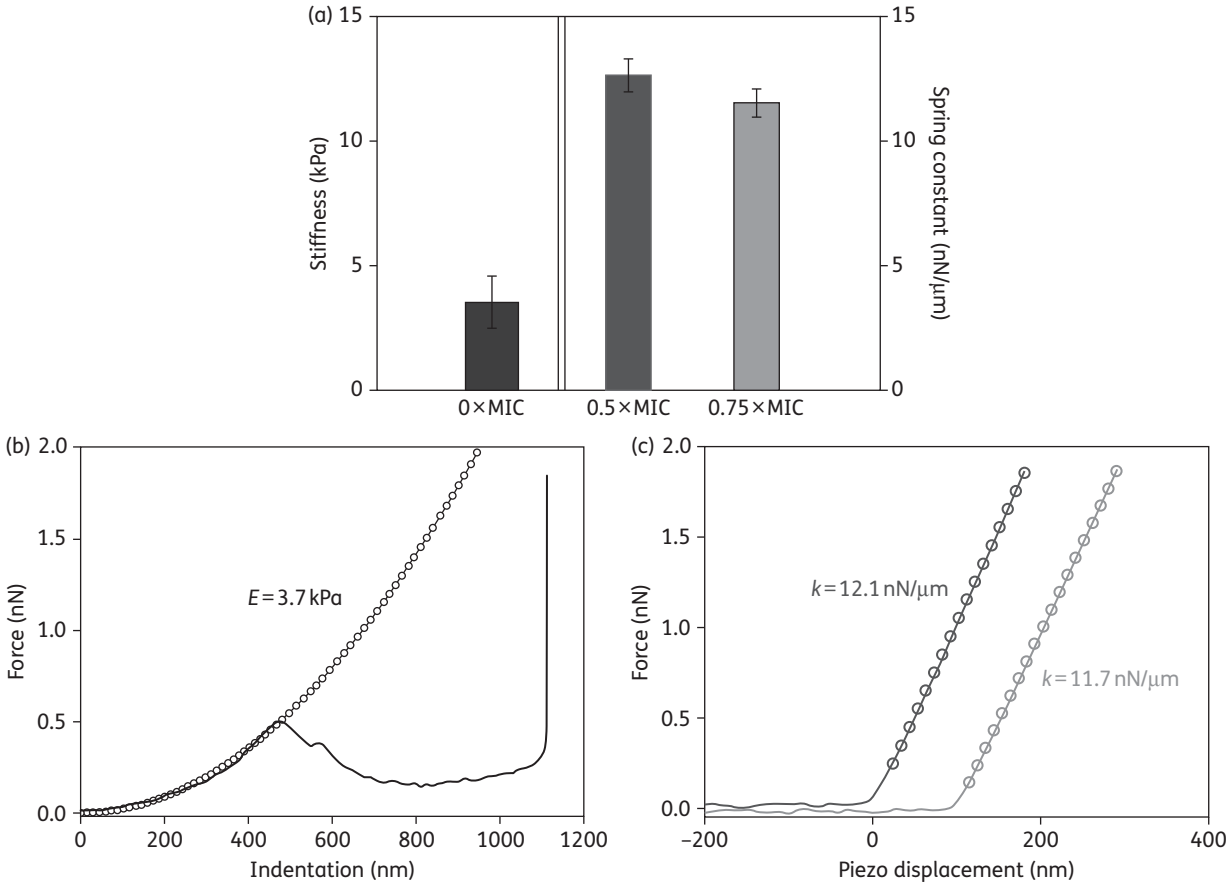

Figure 4. Nanomechanical properties of *K. pneumoniae* ATCC 700603 cells. (a) Histogram presenting the stiffness values measured on cells in native conditions (dark grey bar) and the bacterial spring constants measured on cells treated with colistin at 0.5×MIC (0.25 mg/L; mid-grey bar) or 0.75×MIC (0.375 mg/L; light grey bar). In each case, values were measured on three cells from three independent cultures. (b) Representative indentation curve obtained from the top of a cell in native conditions (grey line), fitted using the Hertz model (circles). (c) Representative force curves obtained for cells treated with colistin at 0.5×MIC (0.25 mg/L; dark grey line) or treated with colistin at 0.75×MIC (0.375 mg/L; light grey line), fitted using the Hooke model (circles).

different from those of force curves recorded on glass slides (Figure S1), we chose to analyse them with the Hooke model, which considers the couple cantilever/cell wall as a spring. This model can be used to obtain the bacterial spring constant, expressed in N/m. Figure 4(c) shows the force curves obtained for cells treated with colistin at 0.5×MIC (0.25 mg/L) and 0.75×MIC (0.375 mg/L), fitted using the Hooke model. The results obtained on five cells from three independent cultures in each case were 12.6 ± 0.7 nN/μm for treatment at 0.5×MIC and 11.5 ± 0.6 nN/μm for treatment at 0.75×MIC. The difference between these two conditions was not significant. These results allow us to conclude that, in native conditions, cells are covered by the capsule, and only the stiffness of this capsule can be measured. However, when cells were treated with colistin, the capsule was removed from the surface, allowing access of the tip to the bacterial cell wall. The cell wall was not soft enough for the tip to indent into it; as we could not compare spring constant values with those of untreated cells, where the cell wall was not accessible, it is impossible to conclude whether the cell wall is naturally stiff, or whether the high stiffness is a result of the colistin treatment.

In the case of the colistin-resistant strain, KpATCCm, the situation was different, since colistin seemed to have no effect on the morphology of the cells (Figure 3). However, extend force curves acquired on cells treated with colistin suggested that the organization of the capsule, visible in native conditions, was lost upon treatment. In native conditions we could fit the first spike of the indentation curve, likely corresponding to the capsule of the cells, using the Hertz model (Figure 5b). The values obtained for five cells from three independent cultures were 21.3 ± 4.2 kPa (Figure 5a). This value, 5-fold higher than that measured on the capsule of the susceptible strain, confirms the previous observation on the difference in capsular organization between the two strains. Since the capsule was still present when cells were treated with colistin, we could then fit the indentation curves obtained for treated cells also using the Hertz model (Figure 5b), and found an increase in average stiffness to 74.4 ± 19.7 kPa when cells were treated with colistin at 0.5×MIC (8 mg/L) and to 88.5 ± 19.4 kPa when cells were treated with colistin at 0.75×MIC (12 mg/L, Figure 5a). Therefore, along with the apparent loss of the capsule organization on the extend force curves (Figure 3) recorded on treated KpATCCm cells, the

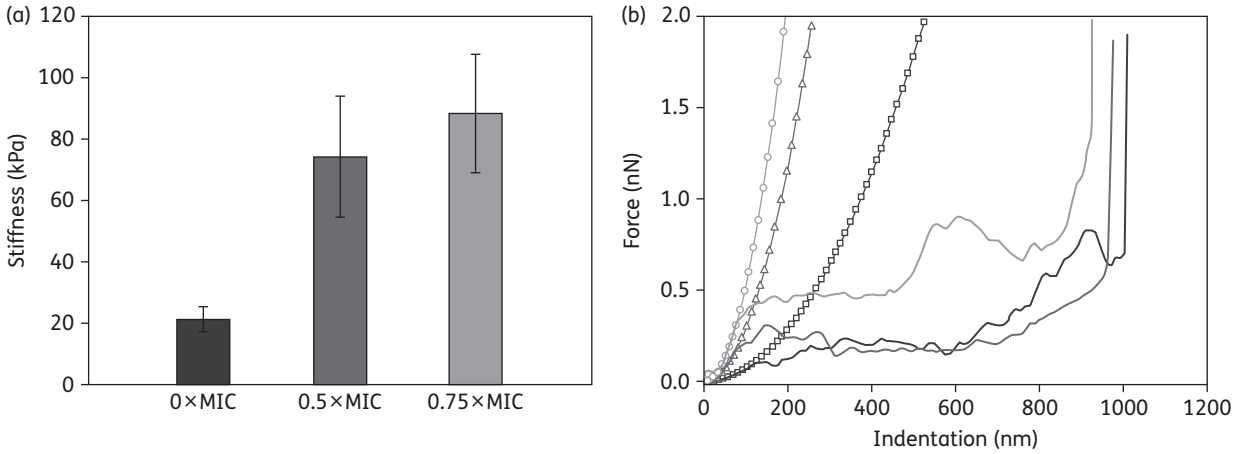

Figure 5. Nanomechanical properties of *K. pneumoniae* colistin-resistant cells. (a) Histogram presenting the stiffness values measured on cells in native conditions (dark grey bar), treated with colistin at 0.5×MIC (8 mg/L; mid-grey bar) or treated with colistin at 0.75×MIC (12 mg/L; light grey bar). In each case, values were measured on three cells from three independent cultures. (b) Representative indentation curves fitted using the Hertz model obtained from the top of a cell in native conditions (dark grey line, Hertz model, squares), treated with colistin at 0.5×MIC (8 mg/L; grey line, Hertz model, triangles) or treated with colistin at 0.75×MIC (12 mg/L; light grey line, Hertz model, circles).

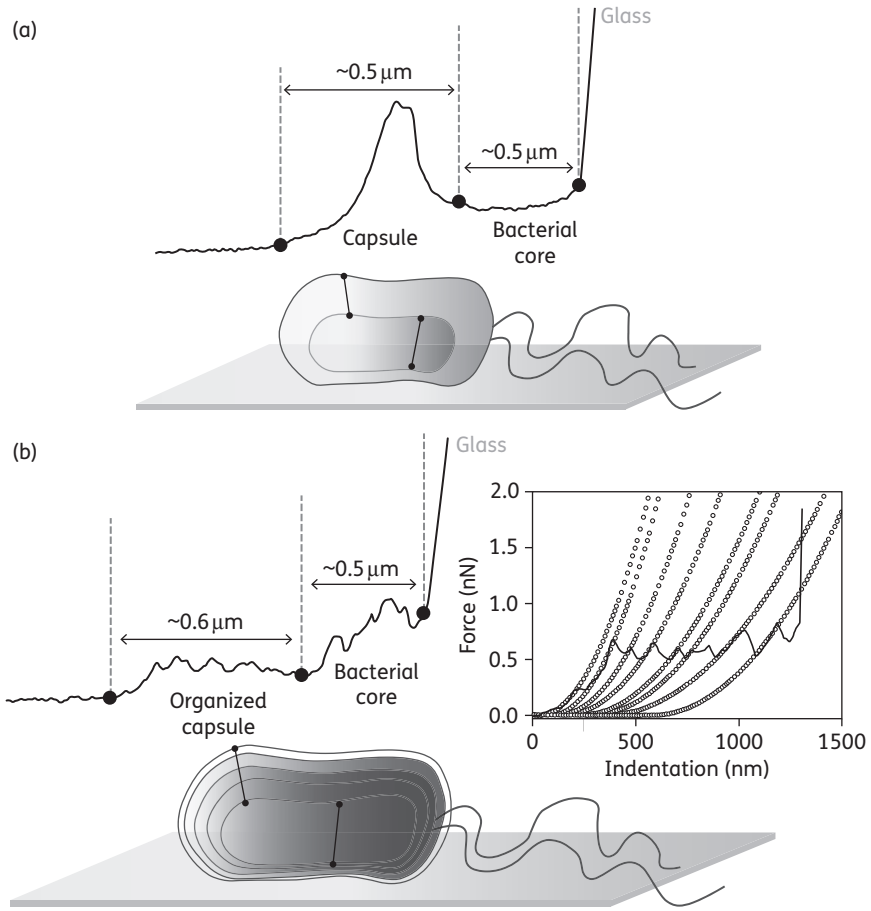

Figure 6. Schematic representation of the hypothesis formulated on capsular architecture. (a) Capsule organization of *K. pneumoniae* ATCC 700603. (b) Capsule organization of colistin-resistant *K. pneumoniae*. The graphic in (b) shows an indentation curve recorded on the top of a colistin-resistant *K. pneumoniae* cell in native conditions (grey line); spikes were fitted using the Hertz model.

nanomechanical data also show that the stiffness of the capsule of the colistin-resistant strain increases upon treatment with colistin.

Discussion

Resistance to colistin is no longer a threat; it is unfortunately a sad reality that modifies the treatment options of patients infected with Gram-negative bacteria (e.g. *Pseudomonas aeruginosa*, *A. baumannii*, *K. pneumoniae* and *Escherichia coli*) already resistant to multiple antibiotics. Although the precise mechanism of action of colistin is still the subject of much discussion, the main mechanism of resistance characterized so far involves the addition of the L-Ara4N moiety to lipid A.[19] In addition, it has been demonstrated that synthesis of the L-Ara4N moiety is strongly dependent on the two-component systems PmrA/PmrB and PhoP/PhoQ.[20,21] Many publications concerned with colistin resistance have clearly shown the pivotal role of these two-component systems in such a mechanism, and it has been demonstrated that these systems are overexpressed in *K. pneumoniae* after exposure to polymyxins.[40] More recent studies have also highlighted the impact of mutations in the *pmrA* and *pmrB* genes[41–43] and the *phoP* and *phoQ* genes.[41] As previous studies have also pointed out the possible role of genes involved in the constitutive synthesis of LPS,[44] we were also interested in the expression of three target genes: *lpxA*, *lpxC* and *msbA*. To determine which of these systems were involved in the colistin-resistant phenotype of the KpATCCm strain, we therefore decided to study the expression of the following nine genes: *lpxA*, *lpxC*, *msbA*, *pmrA*, *pmrB*, *pmrD*, *phoP*, *phoQ* and *arnT*. Our results demonstrated that, whatever the strain considered (i.e. colistin-susceptible KpATCC or colistin-resistant KpATCCm) the expression of these genes was never modified. We also investigated the expression of these genes under colistin pressure in order to determine the impact of colistin concentration on gene expression. Again, we did not observe any changes in gene expression in KpATCCm under colistin pressure, unlike the previous observations of Kim *et al*.[40] Therefore, we decided to look for another mechanism of resistance, which led us to investigate the *mgrB* gene, a recently described factor of colistin resistance. This gene in *K. pneumoniae* encodes a transmembrane protein that exerts negative feedback on the PhoP/PhoQ regulatory system.[23] It was recently discovered that the *mgrB* gene could be mutated by insertional inactivation (e.g. by an IS5-like element and other ISs) in *K. pneumoniae* after colistin exposure.[19,23,24] Indeed, we could identify an insertion in the *mgrB* gene in KpATCCm, but not in KpATCC. The size of this insertion, which we evaluated to be ∼1000 bp, corroborates the size suggested by Olaitan *et al*.[19] Therefore, we can confidently assume that, in KpATCCm, the mutation/inactivation of *mgrB* causes the inactivation of the PhoP/PhoQ and PmrA/PmrB two-component systems, and of the *arnBCADTEF* operon, which is in accordance with previous results obtained by Lippa and Goulian.[45]

This first approach led to the understanding of the genetic cause of the colistin resistance of KpATCCm. It was now of great interest to be able to make the link between these genetic data and the structure and nanomechanical properties of the capsules of the two different strains. Combining these two approaches is not common in the literature,[46] and allowed us in this study to unravel the 'outside' modifications of the capsule caused by an 'inside' gene mutation.

As mentioned earlier, the described mechanism of action of colistin is to interact, due to its strong positive charge, with LPS molecules present on the outer membrane of Gram-negative bacteria, inducing changes in membrane permeability and therefore leading to cell death.[15,47] However, the exact mechanism by which colistin induces bacterial death is still unknown. Some studies have shown that multiple cell targets might be involved, as polymyxin-mediated killing takes place prior to an increase in membrane permeability.[48,49] Also, colistin has been shown to be effective against mycobacterial species, which have a cell wall based on mycolic acid instead of LPS.[50] Thus, LPS might not be the only target of colistin; phospholipids might also be a target. However, in the case of capsulated bacteria, colistin has to interact first with capsular polysaccharides before it can pass through the capsule to reach LPS on the outer membrane, and then the phospholipids of the cytoplasmic membrane. The bacteria are killed as a result of the formation of ion channels, transmembrane pores or membrane ruptures of the cytoplasmic membrane.[48,51]

In our case, we worked on *K. pneumoniae*, a capsulated bacterial species. We compared the capsule organization of a strain susceptible to colistin with a strain resistant to colistin, KpATCCm.

Among others, Campos *et al*.[52] and Llobet *et al*.[53] have also shown that capsular polysaccharides in *K. pneumoniae* are involved in polymyxin resistance, providing a protective shield against polymyxin interactions with the cell surface,[52] or by binding colistin, thereby reducing the amount of colistin reaching the cell surface.[53] However, the amount of capsule polysaccharides must reach a threshold value in order to confer resistance to colistin. Other colistin resistance mechanisms have also been described, such as LPS modification, changes in the negative charge of the outer membrane, and efflux pump systems.[11]

In this study, we observed a previously undescribed capsule phenotype that probably contributes to colistin resistance and can be linked to *mgrB* inactivation. Indeed, as can be seen in Figure 6, force curves recorded on the susceptible strain showed a spike corresponding to the contact and indentation of the AFM tip into the capsular polysaccharide. As the force applied was high, the AFM tip penetrated the capsule (0.5 μm) and then the bacterial core (0.5 μm) before reaching the PEI coating on the glass slide. Similar experiments conducted on bacteria and eukaryotic cells have shown that it is possible to derive, from the force curves obtained from such experiments, the architecture of the different compartments of the cells traversed.[54–56] In the case of the colistin-resistant strain, the extend force curves presented a first spike followed by several condensed spikes over a distance of 0.6 μm before reaching a second spike. Figure 6(b) presents our interpretation of such force curves. The tip first touches and indents into the capsule, but soon meets another layer of polysaccharides, which is broken with a smaller force (small spike), and then another layer, and so on before reaching the bacterial cell. The bacterial core is then traversed for a distance of 0.5 μm by the AFM tip before it reaches the glass slide again. The fact that the force curves showed several ruptures after the first spike allowed us to hypothesize that the capsule is in fact multilayered. To reinforce this hypothesis, an indentation curve recorded on top of a single live cell in native conditions was analysed (graphic in Figure 6b). Every spike observed on this indentation curve was fitted using the Hertz model (open circles). For every fit,

approximately the same stiffness value was extracted (20 kPa), letting us postulate that each small spike corresponds to the rupture of a layer of polysaccharide. Since KpATCCm is resistant to colistin (MIC = 16 mg/L) compared with *K. pneumoniae* ATCC 700603 (MIC = 0.5 mg/L), this multilayered structure of the capsule could be a key factor in colistin resistance in KpATCCm. However, colistin still interacts with the capsular polysaccharides of the KpATCCm strain. Indeed, studies have shown that capsular polysaccharides can differ in chemical composition. Being positively charged, colistin binds to anionic capsules, but not to cationic or uncharged ones.[53] In our case, the nanomechanical data indicate that the capsule of KpATCCm becomes harder (stiffness increases) with increasing concentration of colistin and its organization as several superposed layers is lost. Therefore, colistin has an effect on the nanomechanical properties of the capsule, leading us to think that colistin still interacts with the capsule, but, because of its organization, cannot penetrate it to reach the cytoplasmic membrane of the bacterium.

To conclude, this study describes for the first time, as far as we know, imaging of the capsule of living cells of *K. pneumoniae* by AFM. It also allowed us to show that colistin was able to remove the capsule of a colistin-susceptible strain, but not that of a colistin-resistant strain. Results of force spectroscopy experiments led us to hypothesize a model of colistin resistance based on the nanoarchitecture of the capsule. The colistin-resistant strain presents a well-organized multilayered capsule that may interact with colistin. These results, combined with the genetic data obtained in the first part of the study, showed that inactivation of the *mgrB* gene had direct consequences on the organization of the capsule of the colistin-resistant strain. Our hypothesis for future studies is that the multilayered capsule does not let colistin penetrate to the cell wall to reach its targets. Additional AFM experiments and genetic studies on clinical isolates of colistin-susceptible and -resistant *K. pneumoniae* are needed to further investigate the morphology of the capsule, the impact of colistin exposure on these isolates and, ultimately, the mechanisms of colistin resistance during therapy.

Acknowledgements

E. D. is a researcher of the Centre National de la Recherche Scientifique (CNRS). We thank Marion Grare for performing antibiograms on the two strains used, and Mark D. Adams (Craig Venter Institute, La Jolla, CA, USA) and Jean-Marc Rolain (URMITE CNRS IRD UMR 6236, Marseille, France) for helpful discussions.

Funding

This work has been supported by a grant from 'Young Scientist Program' of ANR (Agence Nationale de la Recherche), project ANR-11-JSV5-001-01, n° (SD) 30 02 43 31. C. F. is supported by a grant from 'Direction Générale de l'Armement' (DGA) for her 3 year PhD study.

Transparency declarations

None to declare.

Supplementary data

Table S1 and Figure S1 are available as Supplementary data at *JAC* Online (http://jac.oxfordjournals.org/).

References

1 Keynan Y, Rubinstein E. The changing face of *Klebsiella pneumoniae* infections in the community. *Int J Antimicrob Agents* 2007; **30**: 385–9.

2 Podschun R, Ullmann U. *Klebsiella* spp. as nosocomial pathogens: epidemiology, taxonomy, typing methods, and pathogenicity factors. *Clin Microbiol Rev* 1998; **11**: 589–603.

3 Gupta A, Ampofo K, Rubenstein D *et al*. Extended spectrum β lactamase-producing *Klebsiella pneumoniae* infections: a review of the literature. *J Perinatol* 2003; **23**: 439–43.

4 Livermore DM. Current epidemiology and growing resistance of Gram-negative pathogens. *Korean J Intern Med* 2012; **27**: 128–42.

5 Jacoby GA, Sutton L. Properties of plasmids responsible for production of extended-spectrum β-lactamases. *Antimicrob Agents Chemother* 1991; **35**: 164–9.

6 Perez F, Endimiani A, Hujer KM *et al*. The continuing challenge of ESBLs. *Curr Opin Pharmacol* 2007; **7**: 459–69.

7 Rasheed JK, Anderson GJ, Yigit H *et al*. Characterization of the extended-spectrum β-lactamase reference strain, *Klebsiella pneumoniae* K6 (ATCC 700603), which produces the novel enzyme SHV-18. *Antimicrob Agents Chemother* 2000; **44**: 2382–8.

8 Pasteran F, Veliz O, Rapoport M *et al*. Sensitive and specific modified Hodge test for KPC and metallo-β-lactamase detection in *Pseudomonas aeruginosa* by use of a novel indicator strain, *Klebsiella pneumoniae* ATCC 700603. *J Clin Microbiol* 2011; **49**: 4301–3.

9 Bush K, Jacoby GA. Updated functional classification of β-lactamases. *Antimicrob Agents Chemother* 2010; **54**: 969–76.

10 Munoz-Price LS, Poirel L, Bonomo RA *et al*. Clinical epidemiology of the global expansion of *Klebsiella pneumoniae* carbapenemases. *Lancet Infect Dis* 2013; **13**: 785–96.

11 Ah Y-M, Kim A-J, Lee J-Y. Colistin resistance in *Klebsiella pneumoniae*. *Int J Antimicrob Agents* 2014; **44**: 8–15.

12 Vaara M. Novel derivatives of polymyxins. *J Antimicrob Chemother* 2013; **68**: 1213–9.

13 Koch-Weser J, Sidel VW, Federman EB *et al*. Adverse effects of sodium colistimethate. Manifestations and specific reaction rates during 317 courses of therapy. *Ann Intern Med* 1970; **72**: 857–68.

14 Nation RL, Li J. Colistin in the 21st century. *Curr Opin Infect Dis* 2009; **22**: 535–43.

15 Yahav D, Farbman L, Leibovici L, Paul M. Colistin: new lessons on an old antibiotic. *Clin Microbiol Infect* 2012; **18**: 18–29.

16 Velkov T, Thompson PE, Nation RL *et al*. Structure–activity relationships of polymyxin antibiotics. *J Med Chem* 2010; **53**: 1898–916.

17 Zhang L, Dhillon P, Yan H *et al*. Interactions of bacterial cationic peptide antibiotics with outer and cytoplasmic membranes of *Pseudomonas aeruginosa*. *Antimicrob Agents Chemother* 2000; **44**: 3317–21.

18 Velkov T, Roberts KD, Nation RL *et al*. Pharmacology of polymyxins: new insights into an 'old' class of antibiotics. *Future Microbiol* 2013; **8**: 711–24.

19 Olaitan AO, Morand S, Rolain J-M. Mechanisms of polymyxin resistance: acquired and intrinsic resistance in bacteria. *Antimicrob Resist Chemother* 2014; **5**: 643.

20 Raetz CRH, Whitfield C. Lipopolysaccharide endotoxins. *Annu Rev Biochem* 2002; **71**: 635–700.

21 Falagas ME, Rafailidis PI, Matthaiou DK. Resistance to polymyxins: mechanisms, frequency and treatment options. *Drug Resist Updat* 2010; **13**: 132–8.

22 Nikaido H. Molecular basis of bacterial outer membrane permeability revisited. *Microbiol Mol Biol Rev* 2003; **67**: 593–656.

23 Cannatelli A, D'Andrea MM, Giani T *et al*. In vivo emergence of colistin resistance in *Klebsiella pneumoniae* producing KPC-type carbapenemases mediated by insertional inactivation of the PhoQ/PhoP mgrB regulator. *Antimicrob Agents Chemother* 2013; **57**: 5521–6.

24 Poirel L, Jayol A, Bontron S *et al*. The *mgrB* gene as a key target for acquired resistance to colistin in *Klebsiella pneumoniae*. *J Antimicrob Chemother* 2015; **70**: 75–80.

25 Binnig G, Quate CF, Gerber C. Atomic force microscope. *Phys Rev Lett* 1986; **56**: 930–4.

26 Müller DJ, Dufrêne YF. Atomic force microscopy: a nanoscopic window on the cell surface. *Trends Cell Biol* 2011; **21**: 461–9.

27 Formosa C, Grare M, Duval RE *et al*. Nanoscale effects of antibiotics on *P. aeruginosa*. *Nanomedicine* 2012; **8**: 12–6.

28 Formosa C, Grare M, Jauvert E *et al*. Nanoscale analysis of the effects of antibiotics and CX1 on a *Pseudomonas aeruginosa* multidrug-resistant strain. *Sci Rep* 2012; **2**: 575.

29 Formosa C, Schiavone M, Martin-Yken H *et al*. Nanoscale effects of caspofungin against two yeast species, *Saccharomyces cerevisiae* and *Candida albicans*. *Antimicrob Agents Chemother* 2013; **57**: 3498–506.

30 El-Kirat-Chatel S, Beaussart A, Alsteens D *et al*. Nanoscale analysis of caspofungin-induced cell surface remodelling in *Candida albicans*. *Nanoscale* 2013; **5**: 1105–15.

31 Soon RL, Nation RL, Harper M *et al*. Effect of colistin exposure and growth phase on the surface properties of live *Acinetobacter baumannii* cells examined by atomic force microscopy. *Int J Antimicrob Agents* 2011; **38**: 493–501.

32 Soon RL, Nation RL, Hartley PG *et al*. Atomic force microscopy investigation of the morphology and topography of colistin-heteroresistant *Acinetobacter baumannii* strains as a function of growth phase and in response to colistin treatment. *Antimicrob Agents Chemother* 2009; **53**: 4979–86.

33 Mortensen NP, Fowlkes JD, Sullivan CJ *et al*. Effects of colistin on surface ultrastructure and nanomechanics of *Pseudomonas aeruginosa* cells. *Langmuir* 2009; **25**: 3728–33.

34 Clinical and Laboratory Standards Institute. *Methods for Dilution Antimicrobial Susceptibility Tests for Bacteria That Grow Aerobically—Eighth Edition: Approved Standard M07-A8*. CLSI, Wayne, PA, USA, 2009.

35 Francius G, Tesson B, Dague E *et al*. Nanostructure and nanomechanics of live *Phaeodactylum tricornutum* morphotypes. *Environ Microbiol* 2008; **10**: 1344–56.

36 Hutter JL, Bechhoefer J. Calibration of atomic-force microscope tips. *Rev Sci Instrum* 1993; **64**: 1868–73.

37 Hertz H. Ueber die Beruhrung fester elastischer Korper. *J Reine Angew Math* 1881; **92**: 156–71.

38 Arnoldi M, Fritz M, Bäuerlein E *et al*. Bacterial turgor pressure can be measured by atomic force microscopy. *Phys Rev E* 2000; **62**: 1034–44.

39 Chopinet L, Formosa C, Rols MP *et al*. Imaging living cells surface and quantifying its properties at high resolution using AFM in QI^{TM} mode. *Micron* 2013; **48**: 26–33.

40 Kim SY, Choi HJ, Ko KS. Differential expression of two-component systems, pmrAB and phoPQ, with different growth phases of *Klebsiella pneumoniae* in the presence or absence of colistin. *Curr Microbiol* 2014; **69**: 37–41.

41 Olaitan AO, Diene SM, Kempf M *et al*. Worldwide emergence of colistin resistance in *Klebsiella pneumoniae* from healthy humans and patients in Lao PDR, Thailand, Israel, Nigeria and France owing to inactivation of the PhoP/PhoQ regulator mgrB: an epidemiological and molecular study. *Int J Antimicrob Agents* 2014; **44**: 500–7.

42 Cannatelli A, Pilato VD, Giani T *et al*. In vivo evolution to colistin resistance by PmrB sensor kinase mutation in KPC-producing *Klebsiella pneumoniae* is associated with low-dosage colistin treatment. *Antimicrob Agents Chemother* 2014; **58**: 4399–403.

43 Jayol A, Poirel L, Brink A *et al*. Resistance to colistin associated with a single amino acid change in protein PmrB among *Klebsiella pneumoniae* isolates of worldwide origin. *Antimicrob Agents Chemother* 2014; **58**: 4762–6.

44 Raetz CRH, Reynolds CM, Trent MS *et al*. Lipid A modification systems in Gram-negative bacteria. *Annu Rev Biochem* 2007; **76**: 295–329.

45 Lippa AM, Goulian M. Feedback inhibition in the PhoQ/PhoP signaling system by a membrane peptide. *PLoS Genet* 2009; **5**: e1000788.

46 Schiavone M, Sieczkowski N, Castex M *et al*. Effects of the strain background and autolysis process on the composition and biophysical properties of the cell wall from two different industrial yeasts. *FEMS Yeast Res* 2015; **15**: 1–11.

47 Bergen PJ, Landersdorfer CB, Zhang J *et al*. Pharmacokinetics and pharmacodynamics of 'old' polymyxins: what is new? *Diagn Microbiol Infect Dis* 2012; **74**: 213–23.

48 Mogi T, Kita K. Gramicidin S and polymyxins: the revival of cationic cyclic peptide antibiotics. *Cell Mol Life Sci* 2009; **66**: 3821–6.

49 Hale JD, Hancock RE. Alternative mechanisms of action of cationic antimicrobial peptides on bacteria. *Expert Rev Anti Infect Ther* 2007; **5**: 951–9.

50 David HL, Rastogi N. Antibacterial action of colistin (polymyxin E) against *Mycobacterium aurum*. *Antimicrob Agents Chemother* 1985; **27**: 701–7.

51 Brogden KA. Antimicrobial peptides: pore formers or metabolic inhibitors in bacteria? *Nat Rev Microbiol* 2005; **3**: 238–50.

52 Campos MA, Vargas MA, Regueiro V *et al*. Capsule polysaccharide mediates bacterial resistance to antimicrobial peptides. *Infect Immun* 2004; **72**: 7107–14.

53 Llobet E, Tomás JM, Bengoechea JA. Capsule polysaccharide is a bacterial decoy for antimicrobial peptides. *Microbiology* 2008; **154**: 3877–86.

54 Liu H, Wen J, Xiao Y *et al*. In situ mechanical characterization of the cell nucleus by atomic force microscopy. *ACS Nano* 2014; **8**: 3821–8.

55 Obataya I, Nakamura C, Han S *et al*. Nanoscale operation of a living cell using an atomic force microscope with a nanoneedle. *Nano Lett* 2005; **5**: 27–30.

56 Suo Z, Avci R, Deliorman M *et al*. Bacteria survive multiple puncturings of their cell walls. *Langmuir ACS J Surf Colloids* 2009; **25**: 4588–94.